

Journal Pre-proofs

Sodium-dependent Glucose Co-Transporter-2 Inhibitor Empagliflozin Exerts Neuroprotective Effects in Rotenone-Induced Parkinson's Disease Model in Zebrafish; Mechanism Involving Ketogenesis and Autophagy

İsmail Ünal, Derya Cansız, Merih Beler, Zehra Sezer, Elif Güzel, Ebru Emekli-Alturfan

PII: S0006-8993(23)00307-4

DOI: <https://doi.org/10.1016/j.brainres.2023.148536>

Reference: BRES 148536

To appear in: *Brain Research*

Received Date: 28 April 2023

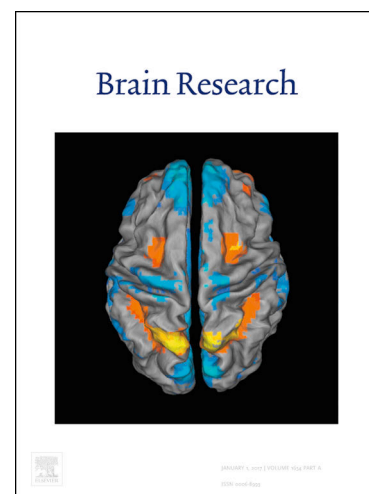
Revised Date: 26 June 2023

Accepted Date: 14 August 2023

Please cite this article as: I. Ünal, D. Cansız, M. Beler, Z. Sezer, E. Güzel, E. Emekli-Alturfan, Sodium-dependent Glucose Co-Transporter-2 Inhibitor Empagliflozin Exerts Neuroprotective Effects in Rotenone-Induced Parkinson's Disease Model in Zebrafish; Mechanism Involving Ketogenesis and Autophagy, *Brain Research* (2023), doi: <https://doi.org/10.1016/j.brainres.2023.148536>

This is a PDF file of an article that has undergone enhancements after acceptance, such as the addition of a cover page and metadata, and formatting for readability, but it is not yet the definitive version of record. This version will undergo additional copyediting, typesetting and review before it is published in its final form, but we are providing this version to give early visibility of the article. Please note that, during the production process, errors may be discovered which could affect the content, and all legal disclaimers that apply to the journal pertain.

© 2023 Published by Elsevier B.V.



Sodium-dependent Glucose Co-Transporter-2 Inhibitor Empagliflozin Exerts Neuroprotective Effects in Rotenone-Induced Parkinson's Disease Model in Zebrafish; Mechanism Involving Ketogenesis and Autophagy

Ismail Ünal¹, Derya Cansız², Merih Beler¹, Zehra Sezer³, Elif Güzel³, Ebru Emekli-Alturfan⁴

¹Marmara University, Institute of Health Sciences, Faculty of Pharmacy, Department of Biochemistry, Istanbul, Turkey

²Department Medipol University, Faculty of Medicine, Medical Biochemistry, Istanbul, Turkey

³University of Health Sciences, Hamidiye Institute of Health Sciences, Department of Molecular Medicine, Istanbul, Turkey

⁴Department of Histology and Embryology, Istanbul University-Cerrahpasa, Cerrahpasa Faculty of Medicine, Istanbul, 34098, Turkey

⁵ Istanbul University-Cerrahpaşa, Faculty of Medicine, Department of Biochemistry, Istanbul, Turkey

⁶ Marmara University, Faculty of Dentistry, Department of Basic Medical Sciences, Istanbul, Turkey

Corresponding Author

Prof. Ebru Emekli-Alturfan (ORCID ID: [0000-0003-2419-8587](https://orcid.org/0000-0003-2419-8587))

Marmara University, Faculty of Dentistry,

Department of Basic Medical Sciences,

Istanbul, Turkey

ebriumekli@yahoo.com

Running Title: Empagliflozin and Parkinson's Disease

Data availability statement Data is available on reasonable request.

Consent to participate: All the authors have agreed for authorship, read and approved the manuscript, and given consent to participate.

Consent for publication: All the authors have agreed for authorship, read and approved the manuscript, and given consent for publication.

Funding: This work was supported by Marmara University Scientific Research and Project Commission Project No: TDK-2022-10377

Declaration of competing interest: All authors declare that they have no competing interests.

Ethics approval statement: The experimental procedures were approved by the Institutional Animal Care and Use Committee of Marmara University (58.2020.mar).

Sodium-dependent Glucose Co-Transporter-2 Inhibitor Empagliflozin Exerts Neuroprotective Effects in Rotenone-Induced Parkinson's Disease Model in Zebrafish; Mechanism Involving Ketogenesis and Autophagy

ABSTRACT

Sodium-dependent glucose co-transporter-2 (SGLT2) inhibitor empagliflozin (EMP), is the new class of oral hypoglycemic agent approved as a treatment for Type 2 diabetes. SGLT2 inhibitors may induce ketogenesis through inhibiting the renal reabsorption of glucose. In recent years, positive effects of ketogenic diets on neurodegenerative diseases such as Parkinson's disease (PD) have been reported by improving autophagy. We aimed to evaluate the effects of EMP treatment as a SGLT2 inhibitor that can mimic the effects of ketogenic diet, in rotenone induced PD model in zebrafish focusing on ketogenesis, autophagy, and molecular pathways related with PD progression including oxidative stress and inflammation. Adult zebrafish were exposed to rotenone and EMP for 30 days. Y-Maze task and locomotor analysis were performed. Neurotransmitter levels were determined by liquid chromatography tandem- mass spectrometry (LC-MS/MS). Lipid peroxidation (LPO), nitric oxide (No), alkaline phosphatase, superoxide dismutase, glutathione, glutathione S-transferase (GST), sialic acid, acetylcholinesterase, and the expressions of autophagy, ketogenesis and PD-related genes were determined. Immunohistochemical staining was performed for the microglial marker L-plastin (Lcp1) and tyrosine hydroxylase (Th). EMP treatment improved DOPAC/DA ratio, Y-Maze task, locomotor activity, expressions of Th and Lcp-1, autophagy and inflammation related (*mTor*, *atg5*, *tnf α* , *sirt1*, *il6*, *tnf α*); PD-related (*lrrk2*, *park2*, *park7*, *pink1*), and ketone metabolism-related genes (*slc16a1b*, *pparag*, and *pparab*), and oxidant-damage in brain in the rotenone group as evidenced by decreased LPO, No, and improved antioxidant molecules. Our results showed beneficial effects of EMP as a SGLT2 inhibitor in neurotoxin-induced PD model in zebrafish. We believe our study, will shed light on the mechanism of the effects of SGLT2 inhibitors, ketogenesis and autophagy in PD.

Key words: Sodium-dependent glucose transporter, empagliflozin, Parkinson's disease, autophagy, ketogenesis

INTRODUCTION

Parkinson's disease (PD) is the second most common neurodegenerative disease and affects 1-2% of elderly people (Zhang et al., 2015). Oxidative stress and mitochondrial dysfunction are shown as the main findings of brain degenerative diseases. Abnormal glucose tolerance is observed in 50-80% of PD patients. Peripheral insulin resistance is usually an early anomaly in the pathogenesis of PD. The fact that the condition is related to the disruption of central insulin signaling suggests that metabolic disorder is an etiological factor (Krikorian et al., 2019). Ketogenic diets (KDs) have similar effects to fasting and are claimed to have therapeutic potential in neurodegenerative diseases (Lange et al., 2019). KD is a high-lipid, low-carbohydrate diet that results in elevated fatty acids, relative calorie restriction, modulation of glycemia, and ketosis (Koh et al., 2020). KD causes changes in body metabolism. During the early stages of feeding with KD, the blood glucose concentration decreases and the insulin/glucagon ratio decreases. Since carbohydrate intake is low, high glucagon concentration causes glycogen breakdown in the liver. As a result of suppression of gluconeogenesis, glucose begins to be insufficient for the body. The primary energy source for the brain is glucose. Therefore, ketone bodies (Acetone, Acetoacetate and beta hydroxybutyrate) are synthesized in the liver mitochondria (ketogenesis) and given to the blood as an alternative energy source in cases where glucose is too low (Paoli et al., 2014).

The sodium/glucose cotransporter (or sodium-dependent glucose transporter, SGLT) is a family of glucose transporters found in the intestinal mucosa (enterocytes) of the small intestine (SGLT1) and the proximal tubule of the nephron (SGLT2). They contribute to the renal reabsorption of glucose (Yokono et al., 2014). It has been shown in human and animal studies that SGLT2 inhibition mimics pro-ketogenic effect and calorie restriction (Ferrannini et al., 2016; Nishimura et al., 2015; Suzuki et al., 2014; Devenny et al., 2012; Inagaki et al. 2014).

Empagliflozin (EMP) is a SGLT2 inhibitor and is a part of the new class of oral hypoglycemic agents. EMP is a highly potent, selective, competitive SGLT2 inhibitor approved as a treatment for Type 2 diabetes in patients with normal renal function (Ndefo et al., 2015).

In our study, we propose an effective mechanism that can mimic the ketogenic diet by using an SGLT2 inhibitor in an experimental PD model. Ketogenic diets trigger autophagy, a crucial process for the removal of damaged proteins or dysfunctional organelles, and also provide energy (Crews vd., 2010). Accordingly, in our study, the ketogenic and autophagic effects of EMP, an SGLT2 inhibitor, in the rotenone-induced PD model are examined in zebrafish.

METHODS

Animals and treatment

Wild-type male/female zebrafish (8-10 months old) (AB/AB strain) were housed in a ZebTEC aquarium rack system (Tecniplast, Italy). Under a light/dark cycle of 14/10 h, zebrafish were kept in disease-free conditions at 27 ± 1 C. Animal experiments were carried out in accordance with the European Communities Council Directive of 24 November 1986 (86/609/EEC). The Institutional Animal Care and Use Committee of Marmara University approved all of the experimental procedures applied in this study. The minimum number of fish required to produce statistically significant results was estimated using power analysis-G*Power 3.1 (<https://www.psych.uni-duesseldorf.de/abteilungen/aap/gpower3/>). By using the significance level ($\alpha = 0.05$), power ($\beta = 0.8$), and the effect size ($f=0,4$ representing a large effect), a minimum of 13 fish was found to be required per experimental group to obtain a statistically significant sample size. Accordingly, fish were divided into four groups randomly, and each group consisted of 15 fish. The control group included vehicle-treated healthy fish. Fish in the rotenone group (R) were exposed to 5 $\mu\text{g/l}$ rotenone (Sigma, USA) which was dissolved in 0.1% dimethyl sulfoxide (DMSO) (Sigma, USA). Fish in the EMP and ROT+EMP groups were exposed to 2,25 mg/L EMP (Santa Cruz SC-482194).

The water in the tanks of control and rotenone-treated groups was changed every 48 h to ensure constant uptake by the zebrafish. Zebrafish were fed commercial fish food (Tetramine) twice a day. Tetramine content is minimum 11% crude oil, 51% crude protein, 2.3% calcium, 1.5% phosphorus, maximum 15% ash, 3% crude fiber and 6.5% moisture. The granule size is 0.36–0.65 mm and its energy is 3.39 kcal / g. Amounts of rotenone was administered according to our previous studies (Unal et al, 2023; Unal et al., 2020; Yurtsever et al., 2020; Cansız et al., 2021). At the end of 4 weeks, locomotor activities were determined. 16-hour fasting blood glucose levels were determined from anesthetized fish. Blood was taken from the area of the dorsal aorta posterior to the anus and down the body axis using a gauge needle as previously described (Dandin et al, 2022; Beler et al, 2022). Then fish were euthanized by decapitation followed by rapid removal of the brain and hepatopancreatic tissues for RNA extraction and biochemical analysis. For the analysis of locomotor activity, biochemical parameters and RT PCR data analysts were blinded for the experimental condition. Experimental design of the study is given in Figure 2.

Y-Maze Task and behavior analyses

Impairments in working memory and cognitive or behavioral flexibility are commonly reported in neurological and neuropsychiatric disorders including PD (Handra et al., 2019). Deficiencies identified in the Y-Maze task, may indicate problems associated with the cholinergic system. The cholinergic system is impaired in PD. The zebrafish Y-Maze analysis memory task is a simple and quick training session for novelty discovery. Fish spend more time in the new arm than in the other arms of the Y-Maze in response to both novelty and spatial memory training/testing intervals. Memory impairments are assessed by the ratios of same arm turns (SAR), alternate arm turns (AAR), and spontaneous change performance (SAP) in the Y-maze (Choi et al., 2019).

In our study zebrafish were tested in a Y-Maze glass aquarium with three arms (5 cm long, 2 cm wide and 14 cm high). By grading the pattern of entries into each arm during the course of the test's five minutes, SAP was visually evaluated. As on overlapped triplet series, alternations were considered as consecutive entry in all three arms.

In order to evaluate features of attention during spontaneously working memory, the AARs and SARs were also assessed for each fish. For the determination of locomotor activities, a rectangular transparent glass tank with dimensions (21 cm x 9 cm x 11 cm) and a volume (1.5 l) was used. Fish were transported in their housing tanks to the behavioral room and habituated to the environment for at least one hour before being transferred from their home tanks to the testing tank. The tests were performed between 1 pm and 4 pm. The water temperature and the lighting conditions of the tank were carefully matched to the home tank's water temperature and lighting conditions. The swimming pattern of each fish was recorded for 5 minutes by a camera mounted above the arena, which was used to start and monitor the experiment video.

Y-maze activity analyses, the average speed, total distance traveled by the fish were analyzed using the Tox-Track program that detects and tracks animals inside closed arenas. The exploration rate was also determined (Rodriguez et al., 2018).

Neurotransmitters analyses

The levels of dopamine and 3,4-dihydroxyphenyl- acetic acid (DOPAC) in brain tissues were determined by liquid chromatography tandem-mass spectrometry (LC-MS/MS) in homogenates filtered from syringe filter. For this purpose, brain tissues were homogenized with 0.4M perchloric acid and homogenates were centrifuged at 13,000 g for 20 min (Wang et al., 2017).

Biochemical analyses

Hepatopancreatic tissues were taken from anesthetized fish and, for each group tissues from four fish were pooled for each biological replicate, and for each biological replicate, three technical replicates were performed. Tissues were homogenized in physiological saline to prepare 10% (w/v) homogenates. After centrifuging briefly the supernatant was separated and used for the biochemical parameters. The method of Lowry (1951) was used to evaluate total protein levels and the results of the biochemical parameters were expressed per protein. Malondialdehyde (MDA) is a lipid peroxidation (LPO) end product and MDA levels were evaluated by using the method of Yagi (1984). The results of LPO were given as nmol MDA/mg protein. The levels of nitric oxide (NO) were determined by using the method of Miranda (2001) by reducing nitrate to nitrite using vanadium (III) chloride and the results were given as nmol NO/mg protein.

The activities of superoxide dismutase (SOD) were evaluated by using riboflavin-sensitized photo-oxidation reaction of o-dianisidine and results were given as U/mg protein (Mylorie et al., 1986). The activity of glutathione-S-transferase (GST) enzyme which catalyzes glutathione's conjugation was measured by spectrophotometer at 340 nm (Habig and Jacoby 1981). Acetylcholinesterase (AChE) activity and alkaline phosphatase (ALP) levels were determined by the methods of Ellman (1961) and Walter and Schült (1974) respectively. Sialic acid levels were determined according to the method of Warren (1959).

For the analysis of ketone bodies, the absorbances of beta hydroxybutyrate and acetoacetate ketone bodies in hepatopancreas were measured colorimetrically at 340 nm using the Sigma-MAK134 coded kit. Obtained absorbances were recorded and beta hydroxybutyrate and acetoacetate levels were calculated with the formula given in the protocol in the kit.

Reverse transcription (cDNA synthesis) and quantitative real-time PCR

For real-time PCR analysis, brain and intestinal tissues from three fish were pooled for each biological replicate for each group and, three technical replicates were performed for each biological replicate. Rneasy Mini Kit and Qiacube (Qiagen, Germany) were used to isolate RNA from each pooled brain and intestinal tissues. RT2 Profiler PCR Arrays (Qiagen, Germany) was used to synthesize single-stranded cDNA. DNA Master SYBR Green kit (Qiagen, Germany) was used for the PCRs. Qiagen Rotor Gene-Q Light Cyclor instrument was used to determine the expression of PD-related genes (*park2*, *park7*, *pink1* and *lrrk2*), ketone metabolism-related genes (*slc16a1b*, *ppar α* , and *ppar β*), autophagy and inflammation related genes (*mTor*, *atg5*, *tnf α* , *sirt1*, *il6*, *tnf α*) transcripts quantified by RT-PCR. List of primers used in the study are given in Table 1. Relative transcript levels were evaluated by

using the Delta-Delta CT (DDCT) method through the normalization of the values to the housekeeping gene, β -actin (Livak and Schmittgen, 2001).

Immunohistochemical examination

Th Immunohistochemistry

To investigate the Th expressions in the dopaminergic neurons of the zebrafish brain, immunostaining of Th was performed. The brain was fixed overnight in 2% paraformaldehyde (PFA) in 0.1 M phosphate buffer (pH 7.4) for up to 24 h at 4 °C. The brains were incubated in 25% sucrose solution (0.1 M phosphate buffer) for 2.5 hours and in 35% sucrose solution for 12 hours at 4°C until they sank. Then, the brains were embedded in sucrose (20 % w/v) – Gelatin (7.5% w/v, Sigma) horizontally and flash-frozen in liquid nitrogen. Serial sections (~5 μ m) were taken using a cryostat, and IHC was applied blindly to 11th sections taken equally from each tissue. First of all, the slides were stored at –20 °C until further use. Brain sections were post-fixed in ice-cold 4% PFA (0.1 M phosphate buffer, pH 7.4) for 8 min at 4°C. The tissue sections were blocked and incubated with mouse monoclonal anti-zebrafish Tyrosine Hydroxylase (TH) antibody (1:4000, #22941; Immunostar, Hudson, USA) for labeling dopaminergic cells overnight at 4°C.

The sections were washed three times for 5 min with TPBS (0.1% Tween) and then, biotinylated secondary antibody (SHP125; ScyTek, West Logan, Utah) was applied for 20 min. Afterward, streptavidin-peroxidase solution (SHP125; ScyTek, West Logan, Utah) was applied to the slides and 3,3'-Diaminobenzidine (DAB) (ACJ500; ScyTek, West Logan, Utah) was used as a chromogen. Subsequently, the sections were counterstained with Mayer's hematoxylin to label the nuclei. The sections were examined and photographed under Olympus BX61 digital microscope (Olympus, Tokyo, Japan) attached with a computerized digital camera and CellSens software (DP72; Olympus, Tokyo, Japan). The images of the diencephalon in each group were captured same adjustments and magnification. The diencephalon region in the zebrafish brain was determined according to Kaslin and Panula (2001) and Bartel et al. (2020). The dopaminergic neurons in the diencephalon region were evaluated, and the numbers of TH-positive cells in equivalent sections (11th) from each group were counted using Qupath software (Version 0.3.2; 2021) (Hein et al., 2021; Mysona et al., 2020; Bankhead et al., 2017).

Lcp1 Immunohistochemistry

In brain tissue, immunolabeling was performed to examine the expression level of Lcp1 protein, a marker of monocyte/macrophage cell lineage (Lelieveld et al., 2022). For IHC analysis, tissue sections were kept in PBS at 37°C for 10 minutes and then embedding medium was removed.

Tissue sections were kept in cold methanol (-20°C) for 10 minutes and washed with T-PBS. Then, tissue sections were blocked at RT with 2% BSA and 1% DMSO solution for 1 hour. After blocking, sections were incubated with lymphocyte cytosolic protein 1 (L-plastin; Lcp1) antibody (1:500, #GTX124420; GeneTex, California, USA) for 16-18 hours at 4°C. After washing, biotinylated secondary antibody solution and horse raddish peroxidase solution (ScyTek: SHP125) were applied to the tissue sections. AEC was used as chromogen for Lcp1 immunostaining. After washing the sections, counterstaining was performed by applying Mayer's hematoxylin for 1 min. After washing, tissue sections were closed with water-based closure medium.

The amount of microglia marker was evaluated immunohistochemically by marking for Lcp1 in brain tissue sections. All sections were examined under an Olympus BX61 light microscope and photographed at the same settings (exposure: 21.75 ms) (CellSens software; DP72; Olympus, Tokyo, Japan). In the brain tissue, the areas around the 3rd ventricle and lateral ventricles were scored at 40X magnification using the Fiji software (Crowe and Yue, 2019; Lelieveld et al., 2022). Positive cells were determined after the 'threshold' command applied to the micrograph of the AEC color channel in the Fiji software, and Lcp1 immunolabeling was scored according to the intensity and intensity of the staining (Gence et al., 2022).

Statistics

All statistical analyses were applied by using GraphPad Prism 9.0 (GraphPad Software, San Diego, USA) and the data were given as the mean \pm standard deviation. The data was compared using one-way ANOVA test which was followed by Tukey's multiple comparison tests. The data obtained were given as the mean \pm standard deviation. p-value less than 0.05 was regarded as significant.

RESULTS

Results of blood glucose, body weight and ketone body analyses

At the end of the 4th week, body weights decreased significantly in the EMP, ROT and ROT+EMP groups when compared to the control group ($p < 0.0001$) (Figure 3A). In addition, body weights in the C, EMP, ROT and ROT+EMP groups decreased significantly at the end of the 4th week compared to the initial values ($p < 0.0001$, $p < 0.05$, $p < 0.05$, and $p < 0.0001$ respectively) (Figure 3B). EMP, ROT and ROT+EMP treatments decreased blood glucose levels significantly ($p < 0.0001$). In addition, EMP treatment in the ROT group decreased blood glucose levels when compared with the ROT group ($p < 0.01$) (Figure 3C).

As SGLT2 inhibitors inhibit the reabsorption of glucose through the proximal renal tubules and cause a shift from using glucose to using lipids, we determined ketone levels to see if SGLT2 inhibitor EMP affected the production of ketones in the liver. EMP treatment increased ketone bodies in liver significantly ($p < 0.0001$). On the other hand, in the ROT group, a significant decrease was observed in the level of ketone bodies ($p < 0.0001$) which was increased by EMP treatment ($p < 0.05$).

Results of neurotransmitters analyses and locomotor activity

DOPAC/DA ratio is considered as a measure of DA turnover. EMP treatment increased DOPAC/DA ratio significantly ($p < 0.0001$) whereas ROT treatment decreased DOPAC/DA ratio significantly ($p < 0.001$). On the other hand, EMP treatment in the ROT group, improved DOPAC/DA ratio significantly compared to the ROT group ($p < 0.0001$) (Figure 4A). As rotenone is a mitochondrial complex 1 inhibitor that is known to increase ROS levels and cause a loss in dopaminergic neurons, we applied locomotor activity analyses to determine whether the movements of the fish were affected. Locomotor activities of the groups are given as average speed (B), distance travelled (C), and exploration rate (D) and in Figure 4. The average speed, distance travelled and exploration rate of the ROT group decreased significantly compared to the control group ($p < 0.0001$, $p < 0.0001$ and $p < 0.001$ respectively). EMP treatment in the rotenone group improved average speed, distance travelled and exploration rate ($p < 0.001$, $p < 0.001$ and $p < 0.0001$ respectively) (Figure 4B-D). Images of trajectory and exploration analysis are also given in Figure 4E.

Results of Y-Maze Task

Spontaneous alternation performance (SAP) was measured visually by scoring the pattern of entries into each arm during the 5 min of the test. The alternate arm returns (AARs) and same arm returns (SARs) were scored for each group in order to assess aspects of attention within spontaneous working memory (Wall and Messier 2002). The percent of SAP, AAR, and SAR are given in Figure 5A, 5B and 5C. Decreased SAP percentages in the ROT group was improved by EMP treatment ($p<0.05$) (Figure 5A). In the EMP group, percentages of AAR was significantly higher than the C, ROT and ROT+EMP groups ($p<0.05$, $p<0.001$, and $p<0.001$ respectively). On the other hand, the dramatically increased percentage of SAR in the ROT group was ameliorated by EMP treatment ($p<0.0001$).

Results of Biochemical Analyses

Oxidative stress plays a key role in the destruction of dopaminergic neurons in PD, leading to nitrate and oxidative damage to critical cellular components. To evaluate the oxidant/antioxidant status in the brain, levels of NO, lipid peroxidation (LPO) and activities of antioxidant enzymes superoxide dismutase (Sod) and glutathione S-transferase (Gst) were determined. Brain LPO increased significantly in the rotenone group ($p<0.001$) ($p<0.0001$ and $p<0.001$ respectively) and EMP treatment decreased LPO significantly ($p<0.0001$) (Figure 6A). The tripeptide, γ -l-glutamyl-l-cysteinyl-glycine known as glutathione (GSH) is a strong antioxidant and superoxide dismutase (Sod) is an antioxidant enzyme that converts superoxide to H_2O_2 (Saravanan et al., 2006). In our study, brain GSH levels and Sod activities decreased significantly in the ROT group ($p<0.001$) and EMP treatment improved GSH levels and Sod activities in brain significantly ($p<0.01$ and $p<0.001$ respectively).

As phase-II detoxification enzymes GSTs have a cytoprotective role by catalyzing the conjugation of reduced glutathione (GSH) with reactive electrophiles (Ozdamar and Can-Eke, 2013). To evaluate the effect of EMP on detoxification metabolism in the case of rotenone toxicity Gst activities in the brain were determined. Brain Gst activities increased significantly in the EMP-treated ($p<0.0001$) and in the ROT+EMP groups ($p<0.0001$) (Figure 6D).

As a signaling molecule nitric oxide (NO) is important in the pathophysiology of inflammation. Under typical physiological circumstances, NO has an anti-inflammatory action; contrarily, NO is regarded as a pro-inflammatory molecule that, when overproduced under abnormal

circumstances, causes inflammation (Sharma et al., 2007). When we measured NO levels in the brain to see whether NO is effective in rotenone-induced neurotoxicity and the effect of EMP, we found significantly increased brain NO levels both in the ROT ($p < 0.01$) and ROT+EMP groups ($p < 0.05$). The effect of EMP on reducing increased NO levels was not statistically significant (Figure 7A).

Sialic acids serve as receptors for pathogens and toxins and control how cells interact with one another as well as their glycoprotein and glycolipid structures and other cell surface components. SA affects brain regeneration as well as plasticity. Vertebrate brain SAs are important regulators that support the appropriate growth, upkeep, and integrity of the nervous system (Schnaar et al., 2014). Similar to CRP, SA levels are increased during inflammatory processes, most likely as a result of increased amounts of acute-phase glycoproteins that have been heavily sialylated (von Versen-Hoeynck et al., 2009). In our study, in the rotenone-induced PD model, we measured brain SA levels to evaluate the effect of EMP treatment on the inflammatory process through SA, which is mostly found in gangliocytes in the brain. We found that while SA levels increased with EMP, they decreased with EMP treatment in the ROT group compared to the EMP group (Figure 7B).

Acetylcholinesterase (AChE), a cholinergic enzyme mainly present in postsynaptic neuromuscular junctions, is necessary for the maintenance of balanced cholinergic and dopaminergic systems, for appropriate basal ganglia function (Zhou et al., 2003). As the abnormality of the brain cholinergic system can be associated with the cognitive dysfunction in neurodegenerative diseases (Kish et al., 1988), we evaluated brain AChE activity to see if the impaired cognitive functions determined through Y-Maze task were confirmed by the AChE activity. Rotenone treatment led to a significant increase in brain AChE activity ($p < 0.001$), which was normalized by EMP treatment in the ROT group ($p < 0.05$). On the other hand, EMP treatment alone led to a significant increase in brain AChE activity ($p < 0.001$) (Figure 5C). Both EMP and ROT treatments led to significant increases in brain AChE activity ($p < 0.001$). On the other hand, in the ROT group EMP treatment decreased AChE activity in brain significantly ($p < 0.05$) (Figure 7C).

Alkaline phosphatase (ALP) is an abundant and important cell surface protein that is also found in soluble form in tissues and in several body fluids, along with blood. We determined ALP activity in brain as ALP has been linked to neurodegeneration, with both plasma and cerebrospinal fluid ALP activity having been linked to damage to the central nervous system (Vardy et al., 2012). Brain ALP activity increased significantly in the ROT group ($p < 0.01$) and

EMP treatment in the ROT group normalized the activity of ALP significantly ($p < 0.05$) (Figure 7D).

Results of Gene Expression Analyses

The expressions *pink1*, *park2*, *park7*, and *lrrk2* were determined as they are associated with mitochondrial functions in PD. The Pink1 is a serine/threonine kinase that is thought to play a role in the mitochondrial response to cellular and oxidative stress (Valente et al., 2004). It is also a key component of the Pink1/parkin pathway, which regulates mitochondrial morphology and function in response to stress (Nuytemans et al., 2010). Park2 facilitates mitochondrial maintenance under physiological conditions (Weihofen et al., 2009) and it may cause defective mitochondria to undergo autophagy (Narendra et al., 2008). Park7 (Dj-1) is H₂O₂-responsive, implying that it functions as an antioxidant and serves as a sensor for oxidative stress (Zhang et al., 2005). Park7, Park2, and Pink1 have been suggested to be part of a new E3 ligase complex (Xiong et al., 2009). Lrrk2 is involved in many different cellular processes to initiate mitophagy in a PINK1/parkin-dependent manner (Wauters et al., 2020). We found significantly increased expressions of brain *pink1*, *park2*, *park7*, and *lrrk2* in the rotenone group compared to the control group ($p < 0.0001$, $p < 0.0001$, $p < 0.001$, $p < 0.0001$ respectively) (Figure 8A-D). EMP treatment in the rotenone group decreased the expressions of *pink1*, *park2*, *park7*, and *lrrk2* ($p < 0.0001$, $p < 0.0001$, $p < 0.05$, $p < 0.0001$) (Figure 8A-D).

The role of autophagy in neurodegenerative diseases is controversial. In order to examine the effect of autophagy in the neurodegenerative process in the case of SGLT inhibition, we determined the expressions of *mTor*, *atg5*, *tnf α* , *sirt1* and *il6* genes involved in the autophagic pathway. The expressions of *atg5*, *tnf α* , *sirt1* and, *il6* increased significantly ($p < 0.0001$, $p < 0.0001$, $p < 0.05$, $p < 0.0001$ respectively) whereas the expression of *mTor* decreased in the ROT group ($p < 0.0001$). EMP treatment in the ROT group decreased *mTor*, *atg5*, *tnf α* and, *il6* expressions ($p < 0.05$, $p < 0.05$, $p < 0.0001$ and $p < 0.001$ respectively) and increased *sirt1* expression ($p < 0.01$) (Figure 9A-D).

Members of the SLC16 gene family including *slc16a1b* encode monocarboxylate transporters and catalyze the transport of ketone bodies across the plasma membrane (Halestrap, 2013). When we examined *slc16a1b* expression to determine whether the transport of ketone bodies is affected in the case of SGLT inhibition, we found that EMP treatment increased *slc16a1b* expression both in the control and in the ROT group ($p < 0.0001$) (Figure 10A). To determine the effect of SGLT inhibition on SGLT gene expression, we examined the expression of *slc5a2*,

SGLT encoding gene in zebrafish (Li et al., 2019), and found increased expression of *slc5a2* both in the control and in the ROT group ($p < 0.0001$) (Figure 10B).

The PPARs are receptors for the peroxisome proliferator-activator. While PPARG is crucial for lipid storage and adipogenesis, PPARA is a lipid metabolism regulator that plays significant roles in the release of energy through lipid breakdown (Den Broeder et al., 2015). In our study, we determined the expressions of *pparag* and *pparab* that encode for PPARG and PPARA respectively, in zebrafish in order to detect possible changes in lipid metabolism in case of rotenone toxicity and to determine the effect of SGLT inhibition on this situation. Although *pparag* expression decreased significantly in the ROT group ($p < 0.01$), increased *pparag* expressions were observed in both EMP treated control and ROT groups ($p < 0.0001$) (Figure 10C). On the other hand, ROT treatment increased *pparab* significantly ($p < 0.01$), and EMP treatments decreased *pparab* expressions both in the control and ROT groups ($p < 0.05$ and $p < 0.0001$, respectively) (Figure 10D).

Results of Tyrosine Hydroxylase (Th) and Lymphocyte cytosolic protein 1 (Lcp1) Immunostaining

Th catalyzes the formation of L-DOPA which is the rate-limiting step in dopamine biosynthesis. This enzyme may thus play a role in the development of PD on multiple levels, as well as being a prospective candidate for generating new treatments for the disease (Haavik and Toska, 1998). Th immunostained cells were evaluated to determine the effect of EMP in the rotenone induced PD in zebrafish (Figure 11). Th immunolabeling in the diencephalon region was scored using Fiji software. When the obtained data are evaluated statistically, a significant decrease was detected in the Th expression level in the ROT group ($p < 0.0001$) which was increased significantly with EMP treatment ($p < 0.01$) (Figure 11).

Lcp1, a microglia marker, was immunohistochemically labeled in order to evaluate the effects of EMP on brain tissue in PD induced zebrafish model. When the data obtained from the immunolabeling of Lcp1 in the areas around the third ventricle and lateral ventricles were analyzed statistically, it was seen that there was a significant difference between the groups. A significant increase was detected in the Lcp1 expression level in the ROT group ($p < 0.0001$), on the other hand EMP treatment in the same group decreased the Lcp1 expressions significantly ($p < 0.01$) (Figure 11).

DISCUSSION

In accordance with the enhanced glycemic control, reduced body weight in clinical trials with EMP, in our study body weight and blood sugar decreased in the rotenone and EMP groups (Tikkanen et al., 2015; Neeland et al., 2016). Decreased body weights in the rotenone given group might be related with the inhibitory effect of rotenone on mitochondrial complex I, likely causing decreased mitochondrial energy supply which is suggested to be a contributing factor in the weight reduction (Heinz et al., 2017). The decrease in weight and blood glucose in the EMP groups is related to the SGLT2 inhibition. By preventing glucose reabsorption from the urine into the proximal tubules, SGLT2 increases the excretion of glucose in the urine (up to around 50%). By this way, SGLT2 inhibitors directly lower body weight by eliminating glucose from the kidneys, which results in calorie loss and hence weight loss (Pratama et al., 2022).

In our study, the increased amount of ketone bodies in the liver with EMP treatment supports the ketogenic effects of EMP. Hormones like glucagon can increase ketogenesis, however insulin is the main hormone that controls this process that regulates the main enzymes in the ketogenic pathway, where a low insulin state triggers the process (Dhillon and Gupta, 2023). Accordingly insulin resistance is shown to be aggravated in PD patients which reduces the expression of DA transporters (Takahashi et al., 1996; Stouffer et al., 2015). Consistent with this, rotenone treatment increased ketone bodies in the liver and as a SGLT inhibitor EMP increased the amount of ketone bodies in the liver. The expression of *slc5a2*, SGLT encoding gene in zebrafish, increased in the EMP given groups as a response to the SGLT2 inhibitor effect of EMP. Increased *slc16a1b* expression both in the EMP treated control and ROT groups indicate the stimulation of ketone bodies transport across the plasma membrane and support the ketogenesis-inducing effects of EMP. Both PPARG and PPARG agonists have been shown to have neuroprotective effects in a PD model induced in rodents (Barbiero et al., 2014). The altered expressions of *pparag* and *pparab* are related with the disruption of lipid metabolism due to ROT toxicity. EMP normalized the decreased *pparag* expression in the ROT group while normalizing the increase in the *pparab* expression in the same group.

Decreased locomotor activity as evidenced by decreased distance travelled, exploration rate and average speed are in consistent with our previous studies in rotenone-induced PD model in zebrafish (Unal et al., 2023; Unal et al., 2020; Yurtsever et al., 2020; Cansız et al., 2021). Reduced DOPAC/DA ratio indicating DA turnover in the rotenone group is in consistent with the findings of Bagchi (1998) who reported reduced DOPAC/DA ratio in mouse striatum in after the administrations of MPP⁺ and MPTP neurotoxin. EMP treatment improved the locomotor activity and DOPAC/DA as a compensatory mechanism for dopaminergic neuronal

loss, through the prevention of dopaminergic damage due to oxidative stress, which is improved by the effect of EMP.

Rotenone exposure results in mitochondrial malfunction and oxidative stress. Rotenone treatment-induced nigrostriatal dopaminergic neurodegeneration leads to the loss of TH-positive neurons, as TH is a rate-limiting enzyme in the production of and marker of dopaminergic neurons. Although dopaminergic neurons are related with the use of dopamine transporter (DAT), DAT levels were not determined in our study as it has been shown that DAT does not mediate rotenone toxicity (Richardson et al., 2005).

EMP treatment ameliorated the deficiencies detected in the Y-Maze task of the rotenone group through the improvement SAP and SAR percentages in the ROT group. Impaired working memory and cognitive or behavioral flexibility are commonly reported in PD and the deficiencies determined in the Y-Maze task regarding memory impairments may indicate problems associated with the cholinergic system (Handra et al., 2019) which is also impaired in PD (Choi et al., 2019).

Oxidative stress may initiate or accelerate DA degeneration (Saravanan et al., 2006). In order to evaluate the relationship between the degeneration of dopaminergic neurons and oxidative stress, we determined LPO and No levels as the markers of oxidative stress and GSH and Sod as the major antioxidants. Confirming our previous reports, rotenone treatment caused increased oxidative stress as evidenced by increased LPO and No and decreased GSH and Sod (Unal et al., 2029; Unal et al., 2023; Unal et al., 2020; Yurtsever et al., 2020; Cansız et al., 2021). When we determined Th expression in brain to analyse the dopaminergic neuron degeneration, we observed reduced Th⁺ cells in the rotenone group suggesting the dopaminergic neuron loss as reported in PD patients. The loss of dopaminergic neurons in the rotenone group was rescued by EMP treatment. On the other hand, increased SOD and GST activities in EMP treated groups are unexpected findings as these enzymes are expected to increase in case of oxidative damage. Stimulation of ketogenesis and autophagy due to SGLT2 inhibition may be the possible mechanisms related with the activation of the antioxidant defence mechanisms.

To determine the effects of rotenone and EMP treatments on mitochondrial functions in PD, we determined the expressions of PD-related genes *lrrk2*, *park2*, *park7*, and *pink1*. *Lrrk2* induces the formation of ROS in cells and mutations of *Lrrk2* induce mitochondrial malfunction (Subramaniam and Chesselet, 2013). On the other hand, *Pink1* protects the neurons from the deleterious effects of ROS and maintains the morphology of mitochondria (Wang et al., 2017).

In our study through the stimulation of the autophagic route by SGLT2 inhibitor, DJ-1 encoded by *park7* protected DA neurons against oxidative stress and mitochondrial malfunction. In the rotenone treated group, the disrupted expressions of PD-related genes, which show their effects through the regulation of mitochondrial functions by maintaining the oxidative balance, were improved by EMP.

The majority of SAs in the brain are found on gangliosides, which are sialoglycolipids. SAs have been demonstrated to support the development of microdomains, cell adhesion, tissue homeostasis, cell motility, chemokine sensing, and growth factor retention. EMP treatment may be suggested to increase brain SA content supporting neuroprotective effects of SGLT2 inhibitors including EMP in CNS (Pawlos et al., 2021).

A significant inflammatory process that stimulates the elimination of pathogens and cell debris as well as the processing of immune complexes is complement activation. Complement activation has been shown to be an important mechanism in neurodegenerative diseases including PD (Loeffler et al., 2006) and complement cascade is inhibited by SAs (Klaus et al., 2021). The increased SA content in the ROT group can be evaluated as a protective mechanism to inhibit the increased complement activation due to rotenone toxicity. Moreover increased Lcp-1 which is a microglial marker that functions in the microglial inflammatory response, also indicate the role of inflammation in the rotenone-induced PD model and we also show the amelioration of inflammation by EMP treatment.

In our study Rotenone treatment increased brain AChE activity, an enzyme responsible for acetylcholine hydrolysis and this was normalized by EMP treatment. Increased AChE activity, has been suggested to indicate an early stage of inflammation which may trigger cholinergic downregulation and support the proinflammatory stage during early immune response (Zivkovic et al., 2023). In our study, increased AChE activity in the rotenone group may be due to the inflammatory process induced by rotenone, as supported by the increased il6 and SA in this group and declined cognitive functions as evidenced by the Y-maze task. The increased AChE activity in the EMP group may be attributed to the modulatory action of EMP as ketogenic diets may decrease oxidative stress and modulate inflammatory status (Pinto et al., 2018).

In our study, increased ALP activity in the brain tissues of rotenone treated fish is in accordance with the study of Vardy et al., (2012) where they reported increased ALP activity in the brain and plasma in Alzheimer's disease, another neurodegenerative disease, which was accompanied by a decrease in cognitive functions. ALP in brain has been suggested to dephosphorylate the hyperphosphorylated tau protein resulting in the continuous calcium

influx leading to neuronal loss (Díaz-Hernández et al., 2010). Although, PD was not thought to be a typical tauopathy initially, new research has revealed more proof regarding the tau pathology in PD (Zhang et al., 2018). In our study, EMP treatment in the rotenone group normalized the increased ALP activity in parallel with the improvement in cognitive functions determined by Y-maze.

Dysregulation of autophagy is a basic defense process that keeps nutritional and energy equilibrium in response to stress, underlying the pathophysiologies of various illnesses. More evidence points to the buildup of aberrant proteins and/or damaged organelles that is frequently seen in neurodegenerative illnesses including PD as a result of dysregulation of autophagy (Lynch-Day et al., 2012). One of the essential elements in regulating the induction of autophagy is the master regulator of nutrition and growth factor signaling known as target of rapamycin (TOR). Ketogenic diet is suggested to improve autophagy through the reduction in the signaling of the mTORC1 protein, a crucial regulator of cell metabolism and a potent inhibitor of autophagy (Liśkiewicz et al., 2021).

In our study, sirt1 expression increased in the ROT group due to the protective mechanism against rotenone toxicity. SIRT1 is a NAD-dependent histone deacetylase that plays an important role in the regulation of metabolism, cancer, aging and development. SIRT1 regulates several transcription factors such as FOXO, tumor suppressor p53 and nuclear factor-kappa B (NF- κ B). It regulates the autophagy-lysosome pathway by deacetylation of autophagy-related genes Atg5, Atg7, Atg8 and FoxO1. Therefore, it has been demonstrated that activation of SIRT1 and autophagy constitutes an important protective mechanism for cell survival under oxidative stress conditions (Ou et al., 2014).

It has been suggested that autophagy activation provides neuroprotection against the ROT-induced Parkinson's model. Time-dependent activation of autophagy in the first 36 hours after ROT administration in the human neuroblastoma cell line SH-SY5Y and a dramatic decrease in the level of autophagy in these cells 48 hours after ROT administration were shown (Xiong et al., 2013). ROT inhibits Akt/mTOR pathway, and activation of Akt/mTOR pathway protects SH-SY5Y cells from ROT damage by inducing autophagy (Zhang et al., 2019). Similarly, while mTOR expression decreased in the ROT group in our study, EMP showed a normalizing effect. mTOR, a serine/threonine kinase, is a master regulator of cellular metabolism. mTOR regulates cell growth and proliferation in response to a wide variety of cues, and the signaling pathway is dysregulated in many human diseases. mTOR also plays a crucial role in regulating autophagy (Laplane et al., 2012). ATG5 is essential for autophagic vesicle formation and also

has different functions including the mitochondrial quality control after oxidative damage (Ye et al., 2018).

The results of our study showed that through the stimulation of ketogenesis and autophagy, EMP improved cognitive and locomotor functions and showed neuroprotective effects by preventing oxidative stress, inflammation and microglial activation against the neurotoxic effects of rotenone. These findings point to the promising effect of ketogenic diets in the nutrition of PD patients by showing the protective effects of activation of ketogenic pathways through SGLT2 inhibition against the development of PD.

Additionally, disruption of the gut-microbiome-brain axis in PD may cause gastrointestinal symptoms, which may then affect the motor system and contribute to the pathogenesis of the disease. We have previously shown dysregulated proteins in the intestines and brain tissues of rotenone-exposed zebrafish through proteomic analysis (Unal et al., 2023). Given that gut microbiota is an essential connection between dietary treatments and host health, it is possible that neuroprotective effects of ketogenic diets are modulated by gut microbiota. Jiang et al. (2023) reported that ketogenic diet changed the gut microbiota, metabolites, and systemic and intestinal inflammation, indicating that the microbiota-gut-brain axis had a role in the neuroprotective impact of ketogenic diets. Therefore the role of gut-brain axis in neuroprotection through the stimulation of ketogenesis and autophagy by SGLT2 inhibitor EMP is a topic worth investigating.

FIGURE LEGENDS

Figure 1: Graphical abstract Created with BioRender.com

Figure 2: Experimental design of the study. Created with BioRender.com

Figure 3: (A) Body weights at week 4, (B) Comparison of body weights in weeks 1-4, (C) Blood glucose levels at week 4 (mg/dL), (D) Ketone bodies in liver, **** $p < 0,0001$; ** $p < 0,01$; * $p < 0,05$. C: Control Group; EMP: Empagliflozin Group; ROT: Rotenone Group; ROT+EMPA: Rotenone+ Empagliflozin Group

Figure 4: Bar graph presentation of (A) DOPAC/DA ratio, (B) average speed (B), (C) distance travelled, (D) exploration rate (E) Images of trajectory and exploration analysis of the groups. Data presented are mean \pm SD. **** $p < 0.0001$, *** $p < 0.001$, * $p < 0.05$. C: Control Group; EMP: Empagliflozin Group; ROT: Rotenone Group; ROT+EMPA: Rotenone+ Empagliflozin Group

Figure 5: Spontaneous alternation performance (SAP), alternate arm returns (AAR) and same arm returns (SAR) percentages of the groups. **** $p < 0,0001$; *** $p < 0,001$; ** $p < 0,01$; * $p < 0,05$. C: Control Group; EMP: Empagliflozin Group; ROT: Rotenone Group; ROT+EMPA: Rotenone+ Empagliflozin Group

Figure 6: (A) Brain lipid peroxidation levels, (B) Glutathione levels, (C) Superoxide dismutase, and (D) Glutathione S-transferase activities of the groups. Data presented are mean \pm SD. Significant difference is indicated by an asterisk. **** $p < 0.0001$, *** $p < 0.001$, ** $p < 0.01$, * $p < 0.05$. C: Control Group; EMP: Empagliflozin Group; ROT: Rotenone Group; ROT+EMPA: Rotenone+ Empagliflozin Group

Figure 7: (A) Brain nitric oxide levels, (B) Sialic acid levels, (C) Acetylcholinesterase (AChE), and (D) Alkaline phosphatase (ALP) activities of the groups. Data presented are mean \pm SD. Significant difference is indicated by an asterisk. **** $p < 0.0001$, *** $p < 0.001$, ** $p < 0.01$, * $p < 0.05$. C: Control Group; EMP: Empagliflozin Group; ROT: Rotenone Group; ROT+EMPA: Rotenone+ Empagliflozin Group

Figure 8: Bar graph presentation of the fold change of brain *pink1* (A), *park2* (B), *park7* (C) and *lrrk2* (D) transcripts quantified by RT-PCR. All RT-PCR results are normalized to β -actin, the house keeping gene and expressed as change from their respective controls. The average values were obtained from three experiments. Data presented are mean \pm SD. **** $p < 0.0001$, *** $p < 0.001$, * $p < 0.05$. C: Control Group; EMP: Empagliflozin Group; ROT: Rotenone Group; ROT+EMPA: Rotenone+ Empagliflozin Group

Figure 9: Bar graph presentation of the fold change of brain *mTor* (A), *atg5* (B), *tnf α* (C), *sirt1* (D), and *il6* (E) transcripts quantified by RT-PCR. All RT-PCR results are normalized to β -actin, the house keeping gene and expressed as change from their respective controls. The average values were obtained from three experiments. Data presented are mean \pm SD. **** $p < 0.0001$, *** $p < 0.001$, ** $p < 0.01$, * $p < 0.05$. C: Control Group; EMP: Empagliflozin Group; ROT: Rotenone Group; ROT+EMPA: Rotenone+ Empagliflozin Group

Figure 10: Bar graph presentation of the fold change of hepatopancreatic *slc16a1b* (A), *slc5a2* (B), *pparag* (C), and *pparab* (D), transcripts quantified by RT-PCR. All RT-PCR results are normalized to β -actin, the house keeping gene and expressed as change from their respective controls. The average values were obtained from three experiments. Data presented are mean \pm SD. **** $p < 0.0001$, *** $p < 0.001$, * $p < 0.05$. C: Control Group; EMP: Empagliflozin Group; ROT: Rotenone Group; ROT+EMPA: Rotenone+ Empagliflozin Group

Figure 11: Photomicrographs of TH labeling dopaminergic neurons (brown color) in the brain regions in Control, EMP, ROT, ROT+EMP groups (n=5). Incubation with antibody diluent (without antibody) revealed no staining (E; negative control). The marked areas in the insets, given at an X4 magnification (bar: 200 μ m) represent the original images. Original magnification X40 (bar: 20 μ m). All images were captured the same adjustments. Graphic (F) shows TH positive cell number. **** $p < 0.0001$, *** $p < 0.001$, ** $p < 0.01$, * $p < 0.05$.

REFERENCES

Barbiero, J. K., Santiago, R. M., Persike, D. S., da Silva Fernandes, M. J., Tonin, F. S., da Cunha, C., et al., (2014). Neuroprotective effects of peroxisome proliferator-activated receptor alpha and gamma agonists in model of parkinsonism induced by intranigral 1-methyl-4-phenyl-1, 2, 3, 6-tetrahydropyridine. *Behavioural brain research*, 274, 390-399.

Bagchi, S.P., (1998) Striatal and Urinary DOPAC/DA Ratio May Indicate a Long-Lasting DA Release Enhancement by MPP⁺ and MPTP. *Neurochem Res* 23, 127–134.

Bankhead, P., Loughrey, M.B., Fernández, J.A., Dombrowski, Y., McArt, D.G., Dunne, P.D., et al., (2017) QuPath: Open source software for digital pathology image analysis. *Sci Rep*,7. doi:10.1038/S41598-017-17204-5.

Bartel, W.P., Van Laar, V.S., Burton, E.A., (2020) Parkinson's disease. *Behav Neural Genet Zebrafish*, 377–412.

Belér, M., Cansız, D., Ünal, İ., Üstündağ, Ü.V., Dandin, E., Ak, E., Alturfan, A.A., Emekli-Alturfan, E. (2022) Bisphenol A reveals its obesogenic effects through disrupting glucose tolerance, oxidant-antioxidant balance, and modulating inflammatory cytokines and fibroblast growth factor in zebrafish. *Toxicol Ind Health* 38:19-28.

Cansız, D., Ünal, İ., Üstündağ, Ü.V., Alturfan, A.A., Altinoz, M.A., Elmacı, İ., Emekli-Alturfan, E., (2021) Caprylic acid ameliorates rotenone induced inflammation and oxidative stress in the gut-brain axis in Zebrafish. *Mol Biol Rep.*,48(6):5259-5273

Choi, H. J., Im, S. J., Park, H. R., Park, S., Kim, C. E., & Ryu, S. (2019). Long-term effects of aripiprazole treatment during adolescence on cognitive function and dopamine D2 receptor expression in neurodevelopmentally normal rats. *Clinical Psychopharmacology and Neuroscience*, 17(3), 400.

Crews, L., Spencer, B., Desplats, P., Patrick, C., Paulino, A., Rockenstein, E., Hansen, L., Adame, A., Galasko, D., Masliah, E., (2010). Selective molecular alterations in the autophagy pathway in patients with Lewy body disease and in models of alpha-synucleinopathy. *PLoS One*. 19; 5(2):e9313.

Crowe, A.R., Yue, W., (2019). Semi-quantitative Determination of Protein Expression using Immunohistochemistry Staining and Analysis: An Integrated Protocol. *BIO-PROTOCOL* 2019;9:e3465. doi:0.21769/BioProtoc.3465.

Dandin, E., Üstündağ, Ü.V., Ünal, İ., Ateş-Kalkan, P.S., Cansız, D., Beler, M., Ak, E., Alturfan, A.A., Emekli-Alturfan, E. (2022) Stevioside ameliorates hyperglycemia and glucose intolerance, in a diet-induced obese zebrafish model, through epigenetic, oxidative stress and inflammatory regulation. *Obes Res Clin Pract* 16:23-29.

Den Broeder, M.J., Kopylova, V.A., Kamminga, L.M., Legler, J., (2015). Zebrafish as a Model to Study the Role of Peroxisome Proliferating-Activated Receptors in Adipogenesis and Obesity. *PPAR Res.*:358029.

Devenny, J. J. Godonis, H. E. Harvey, S. J. Rooney, S. Cullen, M. J. Pelleymounter, M. A., (2012). "Weight loss induced by chronic dapagliflozin treatment is attenuated by compensatory hyperphagia in diet-induced obese (DIO) rats." *Obesity*, 20(8), 1645-1652.

Dhillon, K.K., Gupta, S. *Biochemistry, Ketogenesis*. [Updated 2023 Feb 6]. In: *StatPearls* [Internet]. Treasure Island (FL): StatPearls Publishing; 2023

Díaz-Hernández, M., Gómez-Ramos, A., Rubio, A., Gómez-Villafuertes, R., Naranjo, J.R., Miras-Portugal, M.T., Avila, J., (2010) Tissue-nonspecific alkaline phosphatase promotes the neurotoxicity effect of extracellular tau. *J Biol Chem*;285:32539–32548.

Ellman., (1961) A new and rapid colorimetric determination of acetylcholinesterase activity. *Biochem Pharmacol.*, (61),90145-9.

Ferrannini, E. Baldi, S. Frascerra, S. Astiarraga, B. Heise, T. Bizzotto, R. Mari, A. Pieber, T.R. Muscelli, E., (2016). "Shift to fatty substrate utilization in response to sodium–glucose

cotransporter 2 inhibition in subjects without diabetes and patients with type 2 diabetes.” *Diabetes*, 65(5), 1190-1195.

Habig, W.H., Jacoby, W.B., (1981). Assays for differentiation of glutathion-s- transferases. *Methods Enzymol*, 77:398–405

Handra, C., Coman, O. A., Coman, L., Enache, T., Stoleru, S., Sorescu, A. M., et al., (2019). The connection between different neurotransmitters involved in cognitive processes. *Farmacia*, 67(2), 193-201.

Hein, A.L., Mukherjee, M., Talmon, G.A., Natarajan, S.K., Nordgren, T.M., Lyden, E., et al., (2021). QuPath Digital Immunohistochemical Analysis of Placental Tissue. *J Pathol Inform.* ;12:40.

Gence L, Fernezelian D, Bringart M, Veeren B, Christophe A, Brion F, et al., (2022). *Hypericum lanceolatum* Lam. Medicinal Plant: Potential Toxicity and Therapeutic Effects Based on a Zebrafish Model. *Front Pharmacol*;13. doi:10.3389/FPHAR.2022.832928.

Haavik, J., Toska, K., (1998). Tyrosine hydroxylase and Parkinson's disease. *Mol Neurobiol*.16(3):285-309.

Halestrap, A. P., (2013). The SLC16 gene family–structure, role and regulation in health and disease. *Molecular aspects of medicine*, 34(2-3), 337-349.

Handra, C., Coman, O. A., Coman, L., Enache, T., Stoleru, S., Sorescu, A. M., (2019). The connection between different neurotransmitters involved in cognitive processes. *Farmacia*, 67(2), 193-201.

Heinz, S., Freyberger, A., Lawrenz, B., Schladt, L., Schmuck, G, Ellinger-Ziegelbauer H.,(2017). Mechanistic Investigations of the Mitochondrial Complex I Inhibitor Rotenone in the Context of Pharmacological and Safety Evaluation. *Sci Rep*. 4;7:45465.

Inagaki, N. Kondo, K. Yoshinari, T. Takahashi, N. Susuta, Y. Kuki, H., (2014). “Efficacy and safety of canagliflozin monotherapy in Japanese patients with type 2 diabetes inadequately

controlled with diet and exercise: a 24-week, randomized, double-blind, placebo-controlled, Phase III study.” *Expert opinion on pharmacotherapy*, 15(11), 1501-1515.

Jiang, Z., Wang, X., Zhang, H., Yin, J., Zhao, P., Yin, Q., Wang, Z., (2023) Ketogenic diet protects MPTP-induced mouse model of Parkinson's disease via altering gut microbiota and metabolites. *MedComm*,16;4(3):e268.

Kaslin, J., Panula, P., (2001). Comparative anatomy of the histaminergic and other aminergic systems in zebrafish (*Danio rerio*). *J Comp Neurol*, 440:342–77.

Kish, S.J., Schut, L., Simmons, J., Gilbert, J., Chang, L.J., Rebbetoy M., (1998). Brain acetylcholinesterase activity is markedly reduced in dominantly-inherited olivopontocerebellar atrophy. *J Neurol Neurosurg Psychiatry*, 51(4):544-8.

Klaus, C., Liao, H., Allendorf, D.H., Brown, G.C., Neumann, H., (2021). Sialylation acts as a checkpoint for innate immune responses in the central nervous system. *Glia*. 69(7):1619-1636.

Koh, S. Dupuis, N. Auvin, S., (2020). Ketogenic diet and Neuroinflammation. *Epilepsy Research*, 106454.

Krikorian, R. Shidler, M. D. Summer, S. S. Sullivan, P. G. Duker, A. P. Isaacson, R. S. Espay, A. J. (2019). “Nutritional ketosis for mild cognitive impairment in Parkinson’s disease: A controlled pilot trial.” *Clinical Parkinsonism & Related Disorders*, 1, 41-47.

Lange, K. W. Nakamura, Y. Chen, N. Guo, J. Kanaya, S. Lange, K. M. Li, S. (2019). “Diet and medical foods in Parkinson’s disease.” *Food Science and Human Wellness*, 8(2), 83-95.

Laplante, M., & Sabatini, D. M. (2012). mTOR signaling in growth control and disease. *cell*, 149(2), 274-293.

Lelieveld, L.T., Gerhardt, S., Maas, S., Zwiers, K.C., de Wit, C., Beijik, E.H., et al.,(2022). Consequences of excessive glucosylsphingosine in glucocerebrosidase-deficient zebrafish. *J Lipid Res* 2022;63. doi:10.1016/J.JLR.2022.100199.

- Li, S., Yang, Y., Huang, L., Kong, M., & Yang, Z. (2019). A novel compound heterozygous mutation in SLC5A2 contributes to familial renal glucosuria in a Chinese family, and a review of the relevant literature. *Molecular Medicine Reports*, 19(5), 4364-4376.
- Liśkiewicz, D., Liśkiewicz, A., Grabowski, M., Nowacka-Chmielewska, M.M., Jabłońska, K., Wojakowska, A., Marczak, Ł., Barski, J.J., Małecki, A., (2021). Upregulation of hepatic autophagy under nutritional ketosis. *J Nutr Biochem*. 93:108620
- Livak, K.J., Schmittgen, T.D. (2001). Analysis of relative gene expression data using real-time quantitative PCR and the $2^{-\Delta\Delta CT}$ method. *Methods*, 25,402–408.
- Loeffler DA, Camp DM, Conant SB. (2006). Complement activation in the Parkinson's disease substantia nigra: an immunocytochemical study. *J Neuroinflammation*. 19;3:29.
- Lowry, O.H., Rosebrough, N.J., Farr, A.L., Randall, R.J. (1951). Protein measurement with the Folin phenol reagent. *J Biol Chem*, 193:265–275
- Lynch-Day, M.A., Mao, K., Wang, K., Zhao, M., Klionsky, D.J. (2012). The role of autophagy in Parkinson's disease. *Cold Spring Harb Perspect Med*. 2(4):a009357.
- Miranda, K.M., Espey, M.G., Wink, D.A. (2001). A rapid, simple spectrophotometric method for simultaneous detection of nitrate and nitrite. *Nitric Oxide*, 5:62–71
- Mylorie, A.A., Collins, H., Umbles, C., Kyle, J. (1986). Erythrocyte superoxide dismutase activity and other parameters of copper status in rats ingesting lead acetate. *Toxicol Appl Pharmacol*,82:512–520.
- Mysona, B.A., Segar, S., Hernandez, C., Kim, C., Zhao, J., Mysona, D., et al., (2020). QuPath Automated Analysis of Optic Nerve Degeneration in Brown Norway Rats. *Transl Vis Sci Technol*, 9.
- Ndefo, U. A. Anidiobi, N. O. Basheer, E. Eaton, A. T. (2015). Empagliflozin (Jardiance): a novel SGLT2 inhibitor for the treatment of type-2 diabetes. *Pharmacy and Therapeutics*, 40(6), 364.

Neeland, I.J., McGuire, D.K., Chilton, R., Crowe, S., Lund, S.S., Woerle, H.J., Broedl, U.C., Johansen, O.E. (2016). Empagliflozin reduces body weight and indices of adipose distribution in patients with type 2 diabetes mellitus. *Diab Vasc Dis Res.* 13(2):119-26.

Nishimura, R. Tanaka, Y. Koiwai, K. Inoue, K. Hach, T. Salsali, A. Lund, S.S. Broedl, U. C. (2015). Effect of empagliflozin monotherapy on postprandial glucose and 24-hour glucose variability in Japanese patients with type 2 diabetes mellitus: a randomized, double-blind, placebo-controlled, 4-week study. *Cardiovascular diabetology*, 14(1), 11.

Ou, X., Lee, M. R., Huang, X., Messina-Graham, S., & Broxmeyer, H. E. (2014). SIRT1 positively regulates autophagy and mitochondria function in embryonic stem cells under oxidative stress. *Stem cells*, 32(5), 1183-1194.

Paoli, A., Bianco, A., Damiani, E., Bosco, G. (2014). Ketogenic diet in neuromuscular and neurodegenerative diseases. *Biomed Res Int.* 2014:474296.

Pawlos, A., Broncel, M., Woźniak, E., Gorzelak-Pabiś, P. (2021). Neuroprotective Effect of SGLT2 Inhibitors. *Molecules.* 28;26(23):7213.

Pinto, A., Bonucci, A., Maggi, E., Corsi, M., Businaro, R. (2018). Anti-Oxidant and Anti-Inflammatory Activity of Ketogenic Diet: New Perspectives for Neuroprotection in Alzheimer's Disease. *Antioxidants (Basel).* 28;7(5):63.

Pratama, K.G., Tandarto, K., Hengky, A. (2022) Weight Loss Effect Of Sodium-Glucose Cotransporter-2 (Sglt2) Inhibitors In Patients With Obesity Without Diabetes: A Systematic Review. *Acta Endocrinol (Buchar).* 18(2):216-224.

Richardson JR, Quan Y, Sherer TB, Greenamyre JT, Miller GW. (2005) Paraquat neurotoxicity is distinct from that of MPTP and rotenone. *Toxicol Sci.* 88(1):193-201.

Rodriguez, A., Zhang, H., Klaminder, J., Brodin, T., Andersson, P., & Andersson, M. (2018). ToxTrac: a fast and robust software for tracking organisms, *Methods in Ecology and Evolution*, 9(2018), 460-464.

Schnaar, R.L., Gerardy-Schahn, R., Hildebrandt, H. (2014). Sialic acids in the brain: gangliosides and polysialic acid in nervous system development, stability, disease, and regeneration. *Physiol Rev.* 94(2):461-518.

Sharma, J.N., Al-Omran, A., Parvathy, S.S. Role of nitric oxide in inflammatory diseases. *Inflammopharmacology.* 2007 Dec;15(6):252-9. doi: 10.1007/s10787-007-0013-x.

Stouffer, M.A., Woods, C.A., Patel, J.C., Lee, C.R., Witkovsky, P., Bao, L., et al. (2015). Insulin enhances striatal dopamine release by activating cholinergic interneurons and thereby signals reward. *Nat Commun*, 6:8543.

Subramaniam, S.R., Chesselet, M.F. (2013). Mitochondrial dysfunction and oxidative stress in Parkinson's disease. *Prog Neurobiol*, 106-107,17-32.

Suzuki, M. Takeda, M. Kito, A. Fukazawa, M. Yata, T. Yamamoto, M. Nagata, T. Fukuzawa, T. Yamane, M.Honda, K. Suzuki, Y. Kawabe, Y. (2014). Tofogliflozin, a sodium/glucose cotransporter 2 inhibitor, attenuates body weight gain and fat accumulation in diabetic and obese animal models. *Nutrition & diabetes*, 4(7), e125-e125.

Takahashi, M., Yamada, T., Tooyama, I., Moroo, I., Kimura, H., Yamamoto, T., et al. (1996). Insulin receptor mRNA in the substantia nigra in Parkinson's disease. *Neurosci Lett*, 204:201-204.

Tikkanen, I., Narko, K., Zeller, C., et al.,(2015). Empagliflozin reduces blood pressure in patients with type 2 diabetes and hypertension. *Diabetes Care.* 38: 420–428

Ünal, İ., Cansız, D., Sürmen, M.G., Sürmen, S., Sezer, Z., Beler, M., Üstündağ, Ü.V., Güzel, E., Alturfan, A.A., Emekli-Alturfan, E. (2023). Identification of molecular network of gut-brain axis associated with neuroprotective effects of PPAR δ -ligand erucic acid in rotenone-induced Parkinson's disease model in zebrafish. *Eur J Neurosci.* 57(4):585-606

Ünal, İ., Çalışkan-Ak, E., Üstündağ, Ü.V., Ateş, P.S., Alturfan, A.A., Altinoz, M.A., Elmaci, I., Emekli-Alturfan, E., (2020). Neuroprotective effects of mitoquinone and oleandrin on Parkinson's disease model in zebrafish. *Int J Neurosci* 130(6):574–582 23.

Ünal, İ., Üstündağ, Ü.V., Ateş, P.S., Eğilmezer, G., Alturfan, A.A., Yiğitbaşı, T., Emekli-Alturfan, E., (2019). Rotenone impairs oxidant/antioxidant balance both in brain and intestines in zebrafish. *Int J Neurosci*, 129(4):363–368.

Vardy, E.R., Kellett, K.A., Cocklin, S.L., Hooper, N.M.(2012).Alkaline phosphatase is increased in both brain and plasma in Alzheimer's disease. *Neurodegener Dis.* 9(1):31-7.

Wang, Y., Liu, W., Yang, J., Wang, F., Yizhen, S., Zhong, Z.M., Wang, H., Hu, L.F., Liu, C.F. (2017) Parkinson's disease-like motor and non-motor symptoms in rotenone-treated zebrafish. *Neurotoxicology*, 58:103-109.

Warren L. (1959). The thiobarbituric acid assay of sialic acids. *J Biol Chem.* 234: 1971-1975
Wang Y, Liu W, Yang J, et al. Parkinson's disease-like motor and non-motor symptoms in rotenone-treated zebrafish. *Neurotoxicology*. 2017;58:103–109.

Wall, P.M. and Messier, C. (2002). Infralimbic kappa opioid and muscarinic M1 receptor interactions in the concurrent modulation of anxiety and memory. *Psychopharmacology* 160: 233-244.

Walter, K., Schült, C., (1974). Acid and alkaline phosphatase in serum (two point method) In *Methods of enzymatic Analysis* Ed: Bergmeyer HU, 2nd ed. FL, p.856-886.

von Versen-Hoeynck, F.M., Hubel, C.A., Gallaher, M.J., Gammill, H.S., Powers, R.W. (2009). Plasma levels of inflammatory markers neopterin, sialic acid, and C-reactive protein in pregnancy and preeclampsia. *Am J Hypertens.* 22(6):687-92.

Xiong, N., Xiong, J., Jia, M., Liu, L., Zhang, X., Chen, Z., et al., (2013). The role of autophagy in Parkinson's disease: rotenone-based modeling. *Behavioral and Brain Functions*, 9(1), 1-12.

Yagi, K. (1984). Assay for blood plasma or serum. *Method enzymol.* 105:328–331.

Ye, X., Zhou, X. J., & Zhang, H. (2018). Exploring the role of autophagy-related gene 5 (ATG5) yields important insights into autophagy in autoimmune/autoinflammatory diseases. *Frontiers in immunology*, 9, 2334.

Yokono, M. Takasu, T. Hayashizaki, Y. Mitsuoka, K. Kihara, R. Muramatsu, Y. Miyoshi, S. Tahara, A. Kurosaki, E. Li, Q. Tomiyama, H. Sasamata, M. Shibasaki, M. Uchiyama, Y. (2014). SGLT2 selective inhibitor ipragliflozin reduces body fat mass by increasing fatty acid oxidation in high-fat diet-induced obese rats. *European journal of pharmacology*, 727, 66-74.

Yurtsever, İ., Üstündağ, Ü.V., Ünal, İ., Ateş, P.S., Emekli-Alturfan, E. (2020). Rifampicin decreases neuroinflammation to maintain mitochondrial function and calcium homeostasis in rotenone-treated zebrafish. *Drug Chem Toxicol*, 13:1–8.

Zhang, S. Xiao, Q. Le, W. (2015). Olfactory dysfunction and neurotransmitter disturbance in olfactory bulb of transgenic mice expressing human A53T mutant alpha-synuclein. *PLoS One*, 10, e0119928.

Zhang, Y., Guo, H., Guo, X., Ge, D., Shi, Y., Lu, X., et al., (2019). Involvement of Akt/mTOR in the neurotoxicity of rotenone-induced Parkinson's disease models. *International journal of environmental research and public health*, 16(20), 3811.

Zhang, X., Gao, F., Wang, D., Li, C., Fu, Y, He, W., Zhang, J. (2018). Tau Pathology in Parkinson's Disease. *Front Neurol*. 2;9:809.

Zivkovic, A.R., Paul, G.M., Hofer, S., Schmidt, K., Brenner T, Weigand MA, Decker SO. (2023). Increased Enzymatic Activity of Acetylcholinesterase Indicates the Severity of the Sterile Inflammation and Predicts Patient Outcome following Traumatic Injury. *Biomolecules*. 31;13(2):267.

Conceptualization: Ebru Emekli-Alturfan

Data curation: İsmail Ünal, Ebru Emekli-Alturfan

Formal analysis: İsmail Ünal, Ebru Emekli-Alturfan

Funding acquisition: Ebru Emekli-Alturfan

Methodology: İsmail Ünal, Derya Cansız, Merih Beler, Zehra Sezer, Elif Güzel

Supervision: Ebru Emekli-Alturfan

Writing - review & editing: İsmail Ünal, Ebru Emekli-Alturfan

SGLT2 inhibitor empagliflozin increased ketone bodies in zebrafish.

Empagliflozin induced autophagy, improved oxidative stress, and inflammation in PD.

Empagliflozin improved cognitive and locomotor functions in rotenon-induced PD model.

Empagliflozin ameliorated Th and inhibited Lcp-1 expression in rotenon-induced PD model.

Table 1: Forward and reverse primers used in the study.

| | Primers (Forward/Reverse) |
|----------------|---|
| <i>B actin</i> | 5' AAGCAGGAGTACGATGAGTCTG-3' 5'-GGTAAACGCTTCTGGAATGAC-3' |
| <i>pink1</i> | 5'-GGCAATGAAGAT GATGTGGAAC-3' 5'-GGTCGGCAGGAC ATCAGGA-3' |
| <i>park2</i> | 5'- GCGAGTGTGTCT GAGCTGAA-3' |

| | |
|-----------------|--------------------------------|
| <i>park7</i> | 5'-CACACTGGAACA CCAGCACT-3' |
| | 5'-GGCCGGTAAAAGAGCGTTAG-3' |
| | 5'-ACCCATGAGTCCTCCACTA-3' |
| <i>lrrk2</i> | 5'-CCCTAAACCGCA GAGTATCA-3' |
| | 5'-ATTCATAGTCCA CCGGTCTG-3' |
| <i>mTor</i> | 5'-GAAGGCAGACGACATGCAGC-3' |
| | 5'-CAGATACTGCGCCCTCACGA-3' |
| <i>atg5</i> | 5'-TGGTGTTGTTACCAGCTCCAAAG-3' |
| | 5'-ACAGTGTGAAACAGGCGGGT-3' |
| <i>tnfa</i> | 5'-GCTGGATCTTCAAAGTCGGGTGTA-3' |
| | 5'-TGTGAGTCTCAGCACACTTCCATC-3' |
| <i>sirt1</i> | 5'-GCTGGAGGAGCCGAATCTGT-3' |
| | 5'-TGCACCGTTTTTCCTCCACCT-3' |
| <i>il6</i> | 5'-TCAACTTCTCCAGCGTGATG-3' |
| | 5'-TCTTTCCCTCTTTTCCTCCTG-3' |
| <i>slc16a1b</i> | 5'-ACAACCGGGCTGGTGAATGA-3' |
| | 5'-GGAGTGTAGCCCCTGGACC-3' |
| <i>slc5a2</i> | 5'-CATCGCTGGAGCCTTTGTCC-3' |
| | 5'-AAGGCATCCTCTCGTGGCAT-3' |
| <i>pparag</i> | 5'-TATGGTGGACACGCAGACGTT-3' |
| | 5'-GTCCATCATGTGCGGGGTTG-3' |
| <i>pparab</i> | 5'-GACAGTGCGCTGTTCGTCAG-3' |
| | 5'-CACCGGGCAACCGTAAACAC-3' |

